Journal of Computational Mathematics, Vol.25, No.4, 2007, 430–439.

EDGE-ORIENTED HEXAGONAL ELEMENTS *1)

Chao Yang and Jiachang Sun
(*Parallel Computing Lab., Institute of Software, Chinese Academy of Sciences, Beijing 100080, China*
Email: yc@mail.rdcps.ac.cn, sun@mail.rdcps.ac.cn)

Abstract

In this paper, two new nonconforming hexagonal elements are presented, which are based on the trilinear function space $Q_1^{(3)}$ and are edge-oriented, analogical to the case of the rotated Q_1 quadrilateral element. A priori error estimates are given to show that the new elements achieve first-order accuracy in the energy norm and second-order accuracy in the L^2 norm. This theoretical result is confirmed by the numerical tests.

Mathematics subject classification: 65N15, 65N30.
Key words: Nonconforming finite element method, Hexagonal element, Q_1 element.

1. Introduction

The finite element method (FEM) is a powerful tool, which can be easily applied to a large variety of engineering applications. In two dimensions, classical FEMs often treat meshes consisting of triangles, quadrilaterals, etc. While as is well-known, hexagons also extensively exist in the nature as well as in some special application fields, such as in material sciences and nuclear engineering [3, 12, 13]. Moreover, besides triangles and quadrilaterals, only hexagons can form a regular tessellation of the plane [4], which inspires us to consider hexagonal elements.

Noticing that a bivariate quadratic polynomial has six degree of freedoms, one may ask whether the six vertices of a hexagon exactly determine a bivariate quadratic polynomial. Unfortunately, the resulting equation is not unisolvable in general, since the six vertices of the regular hexagon belong to a same quadratic curve, a circle. To construct conforming hexagonal elements avoiding polynomial spaces, some works based on rational function spaces have been carried out in [10, 12, 13, 17]. Moreover, while the nonconforming triangular and quadrilateral elements are well studied, see, e.g., [7, 11, 14, 15, 16], their hexagonal counterparts are less complete. This motivates us to study nonconforming hexagonal elements.

The main goal of this paper is to generalize the quadrilateral rotated Q_1 element [14] to the hexagonal case. We use the so-called three-directional coordinates [18] to explore the symmetry of a hexagon. Two new elements are constructed, both of which are based on trilinear function space $Q_1^{(3)}$ and are edge-oriented. The modified version has an extra degree of freedom on the element face, which is similar to the five-node element proposed by Han in [11]. Optimal order error estimates are given with respect to the energy norm and the L^2 norm. Numerical experiments are presented to demonstrate the accuracy of the proposed method.

Before the end of this section, we recall some notations (or refer to [1, 2]). Let $(\cdot,\cdot)$ denote the L^2 inner product and $||\cdot||_{H^p(\Omega)}$ (resp. $|\cdot|_{H^p(\Omega)}$) be the norm (resp. semi-norm) for the Sobolev space $H^p(\Omega)$.

* Received July 3, 2006; final revised August 14, 2006; accepted December 5, 2006.
1) The research is supported by National Basic Research Program of China (No. 2005CB321702) and National Natural Science Foundation of China (No. 10431050).

2. Nonconforming Hexagonal Element

To begin, we introduce the three-directional coordinates with which the symmetries of a regular hexagon $\widehat{H}$ could be well embodied. As is well-known, under Cartesian coordinates, a plane can be viewed as $\{(t_1, t_2, t_3) \mid t_3 = 0\}$ in the space. While under the three-directional coordinates, the plane $S = \{(t_1, t_2, t_3) \mid t_1 + t_2 + t_3 = 0\}$ are studied. For more details, we refer to [18]. Thus any point in the plane S can be represented by a coordinates triple (t_1, t_2, t_3) with $t_1 + t_2 + t_3 = 0$. A natural coordinates transform between Cartesian coordinates and three-directional coordinates can be

$$\begin{cases} \xi = \dfrac{1}{2}(t_3 - t_2), \\ \\ \eta = \dfrac{\sqrt{3}}{2} t_1, \end{cases} \quad \text{and} \quad \begin{cases} t_1 = \dfrac{2}{\sqrt{3}}\eta, \\ t_2 = -\xi - \dfrac{1}{\sqrt{3}}\eta, \\ t_3 = \xi - \dfrac{1}{\sqrt{3}}\eta. \end{cases}$$

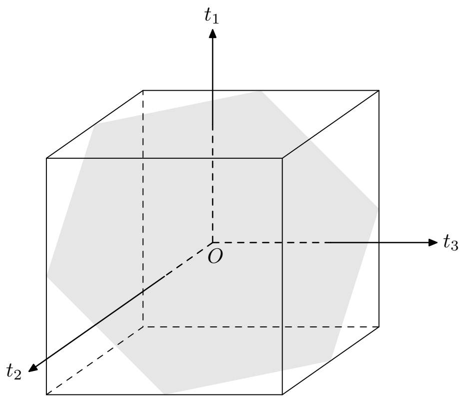

Fig. 2.1. Getting a regular hexagon from a unit-cube.

We let $B = \{(t_1, t_2, t_3) \mid -1 < t_1, t_2, t_3 < 1\}$ be a box domain in the space. Then as illustrated in Fig. 2.1, the regular hexagon $\widehat{H}$ can be easily obtained by letting $\widehat{H} = B \cap S$. Denote the trilinear space over $\widehat{H}$ as

$$Q_1^{(3)}(\widehat{H}) = \text{span}\{1,\ t_1,\ t_2,\ t_3,\ t_2t_3,\ t_3t_1,\ t_1t_2,\ t_1t_2t_3\};$$

obviously we have $\dim(Q_1^{(3)}(\widehat{H})) = 2^3 - 1 = 7$.

We refer symmetric parallel hexagons as an affine-equivalence class of the regular hexagon. For a symmetric parallel hexagon, any two opposite sides are parallel and the three main diagonals meet at one symmetric point, see Fig. 2.2.

For simplicity, assume that Ω is a polygon domain and $\mathcal{T}_h$ be a decomposition of Ω consisted by symmetric parallel hexagons and triangles, where $h = \max_{K \in \mathcal{T}_h} \text{diam} K$. By $\partial \mathcal{T}_h$ we denote the set of all edges F of the element $K \in \mathcal{T}_h$. Assume $\mathcal{T}_h$ satisfies the usual "quasi-uniform" condition [1, 2]. Accordingly, the generic constant C used below is always independent of h. We take the unit regular hexagon $\widehat{H}$ and the unit equilateral triangle $\widehat{T}$ as the reference element. For any $K \in \mathcal{T}_h$, there exists a unique and invertible affine map $F_K : \widehat{K} \to K$, $F_K = B_K \widehat{x} + b_K := x$, where $\widehat{K}$ could be $\widehat{H}$ or $\widehat{T}$.

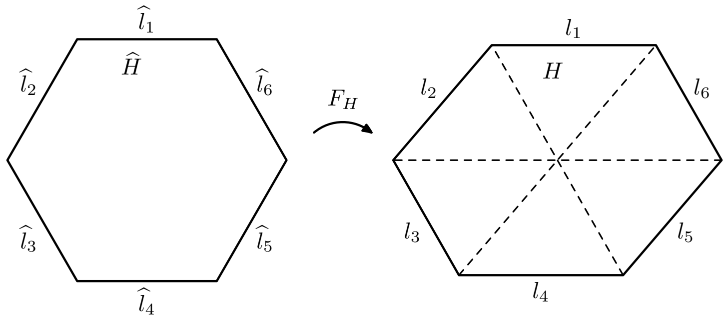

Fig. 2.2. A symmetric parallel hexagon H can be transformed from the regular hexagon $\widehat{H}$ via affine map F_H.

Here we formally define the average and the residual of any function $v \in L^2(M)$ over M by

$$P_0^M(v) = \frac{1}{\text{meas}(M)}(\int_M v d\sigma)$$

and $R_0^M(v) = v - P_0^M(v)$, respectively, where $M \in \mathcal{T}_h$ or $M \in \partial\mathcal{T}_h$. It is easy to see that $P_0^M : L^2(M) \to P_0(M)$ is an orthogonal projection.

Now we try to construct a finite element space where any functions in it are continuous regarding P_0^F over element edge F. For any triangle $T \in \mathcal{T}_h$, it is obvious that we can choose the Crouzeix-Raviart element [7, 2, 1], which has linear shape space and is midpoint-oriented (as well as edge-oriented). For any symmetric parallel hexagon $H \in \mathcal{T}_h$, there exist an affine map F_H that $H = F_H(\widehat{H})$. Thus the shape space $\mathcal{P}$ of H can be determined by the shape space $\widehat{\mathcal{P}}$ of $\widehat{H}$ via $\mathcal{P} = \{q \circ F_H^{-1} :\ q \in \widehat{\mathcal{P}}\}$.

2.1. Q_1 hexagonal element

If we choose the local interpolant operator $\widehat{\Pi}$ on the reference element $\widehat{H}$ under interpolation condition

$$(a): \quad \widehat{\mathcal{N}}^{(a)} = \{P_0^{\widehat{l}_i},\ i = 1, \cdots, 6\},$$

where $\widehat{l}_i,\ i = 1, \cdots, 6$ are the six edges of $\widehat{H}$, then we need to find a suitable subspace $\widehat{\mathcal{P}}^{(a)} \subset Q_1^{(3)}(\widehat{H})$, and $\dim(\widehat{\mathcal{P}}^{(a)}) = 6$. Denote $\{\widehat{\phi}_j\}_{j=1}^6$ as the basis for $\widehat{\mathcal{P}}^{(a)}$ dual to $\widehat{\mathcal{N}}^{(a)}$, then $P_0^{\widehat{l}_i}(\widehat{\phi}_j) = \delta_{ij},\ i, j = 1, \cdots, 6$. An undetermined coefficients method straightforwardly yields

$$\begin{cases} \widehat{\phi}_1 = \frac{3}{8} + \frac{1}{3}t_1 + \frac{3}{4}t_2t_3 + t_1t_2t_3 + c_1\widehat{\phi}_0, \\ \widehat{\phi}_2 = \frac{3}{8} - \frac{1}{3}t_3 + \frac{3}{4}t_1t_2 - t_1t_2t_3 + c_2\widehat{\phi}_0, \\ \widehat{\phi}_3 = \frac{3}{8} + \frac{1}{3}t_2 + \frac{3}{4}t_3t_1 + t_1t_2t_3 + c_3\widehat{\phi}_0, \\ \widehat{\phi}_4 = \frac{3}{8} - \frac{1}{3}t_1 + \frac{3}{4}t_2t_3 - t_1t_2t_3 + c_4\widehat{\phi}_0, \\ \widehat{\phi}_5 = \frac{3}{8} + \frac{1}{3}t_3 + \frac{3}{4}t_1t_2 + t_1t_2t_3 + c_5\widehat{\phi}_0, \\ \widehat{\phi}_6 = \frac{3}{8} - \frac{1}{3}t_2 + \frac{3}{4}t_3t_1 - t_1t_2t_3 + c_6\widehat{\phi}_0, \end{cases}$$

where $\widehat{\phi}_0 = \frac{5}{6} + t_2t_3 + t_3t_1 + t_1t_2$. It is easy to verify that $P_0^{\widehat{l}_i}(\widehat{\phi}_0) = 0$ for all $i = 1, \cdots, 6$.

For the sake of symmetry, we take $c_i \equiv c,\ i = 1, \cdots, 6$. Thus the partition of unity property $\sum_{j=1}^6 \widehat{\phi}_j = 1$ leads to $c = -\frac{1}{4}$. An important observation is that $c = -\frac{1}{4}$ insures the summation of the coefficients of term t_2t_3, t_3t_1, t_1t_2 of any function in $\widehat{\mathcal{P}}^{(a)}$ to be zero. Since

$$\alpha_1t_2t_3 + \alpha_2t_3t_1 - (\alpha_1 + \alpha_2)t_1t_2 = \alpha_1(t_1^2 - t_3^2) + \alpha_2(t_2^2 - t_3^2)$$

for any constant α_j $(j=1,2)$, we eventually get

$$\widehat{\mathcal{P}}^{(a)} = \mathrm{span}\{1,\ t_1,\ t_2,\ t_1^2-t_3^2,\ t_2^2-t_3^2,\ t_1t_2t_3\}. \tag{2.1}$$

2.2. Modified Q_1 hexagonal element

In [11], Han proposes a five-node quadrilateral element by adding an extra degree of freedom on the element face. Here we follow Han's idea by letting

$$(b):\quad \widehat{\mathcal{N}}^{(b)} = \{P_0^{\widehat{l}_i},\ i=1,\cdots,6\}\cup\{P_0^{\widehat{H}}\},\quad \widehat{\mathcal{P}}^{(b)} = Q_1^{(3)}(\widehat{H}).$$

Denote $\{\widehat{\psi}_j\}_{j=1}^7$ as the basis for $\widehat{\mathcal{P}}^{(b)}$, a similar derivation as in Section 2.1 leads to

$$\begin{cases} \widehat{\psi}_1 = -\frac{1}{6}+\frac{1}{3}t_1+\frac{1}{10}t_2t_3-\frac{13}{20}t_3t_1-\frac{13}{20}t_1t_2+t_1t_2t_3, \\ \widehat{\psi}_2 = -\frac{1}{6}-\frac{1}{3}t_3-\frac{13}{20}t_2t_3-\frac{13}{20}t_3t_1+\frac{1}{10}t_1t_2-t_1t_2t_3, \\ \widehat{\psi}_3 = -\frac{1}{6}+\frac{1}{3}t_2-\frac{13}{20}t_2t_3+\frac{1}{10}t_3t_1-\frac{13}{20}t_1t_2+t_1t_2t_3, \\ \widehat{\psi}_4 = -\frac{1}{6}-\frac{1}{3}t_1+\frac{1}{10}t_2t_3-\frac{13}{20}t_3t_1-\frac{13}{20}t_1t_2-t_1t_2t_3, \\ \widehat{\psi}_5 = -\frac{1}{6}+\frac{1}{3}t_3-\frac{13}{20}t_2t_3-\frac{13}{20}t_3t_1+\frac{1}{10}t_1t_2+t_1t_2t_3, \\ \widehat{\psi}_6 = -\frac{1}{6}-\frac{1}{3}t_2-\frac{13}{20}t_2t_3+\frac{1}{10}t_3t_1-\frac{13}{20}t_1t_2-t_1t_2t_3, \\ \widehat{\psi}_7 = 2+\frac{12}{5}(t_2t_3+t_3t_1+t_1t_2). \end{cases}$$

Now, we have constructed two different finite element spaces

$$V_h^{(a/b)} = \big\{v\in L^2(\Omega)\ \big|\ v\circ F_K\in\widehat{\mathcal{P}}^{(a/b)},\ \forall K\in\mathcal{T}_h;\ \ v \text{ is continuous regarding } P_0^F(\cdot), \\ \forall F\in\partial\mathcal{T}_h;\ \text{ and }\ P_0^F(v)=0,\ \forall F\subset\partial\Omega\big\}.$$

3. Error Estimates

For convenience, we consider the following Poisson problem

$$\begin{cases} -\Delta u = f, & \text{in } \Omega, \\ u=0, & \text{on } \partial\Omega. \end{cases} \tag{3.1}$$

Then the weak form of equation (3.1) reads

$$\text{Find } u\in H_0^1(\Omega),\ \text{ such that }\ a(u,v)=(f,v),\quad \forall v\in H_0^1(\Omega), \tag{3.2}$$

where

$$a(u,v)=\int_\Omega \nabla u\cdot\nabla v d\sigma.$$

The approximation of (3.2) is given by

$$\text{Find } u_h\in V_h,\ \text{ such that }\ a_h(u_h,v_h)=(f,v_h),\quad \forall v_h\in V_h, \tag{3.3}$$

with

$$a_h(u_h,v_h)=\sum_{K\in\mathcal{T}_h}\int_K \nabla u_h\cdot\nabla v_h d\sigma.$$

The energy norm induced by $a_h(\cdot,\cdot)$ is

$$||\cdot||_h = (\sum_{K\in\mathcal{T}_h}|\cdot|_{H^1(K)}^2)^{\frac{1}{2}}.$$

It is obvious that $||\cdot||_h$ is a norm on V_h.

Assume $u \in H_0^1(\Omega) \cap H^2(\Omega)$ and $u_h \in V_h$ to be the unique solution of (3.2) and (3.3), respectively. Then the second Strang's Lemma (see [2]) gives

$$||u-u_h||_h \le C\{\inf_{v_h\in V_h} ||u-v_h||_h + \sup_{w_h\in V_h\setminus\{0\}} \frac{|a_h(u-u_h,w_h)|}{||w_h||_h}\}. \tag{3.4}$$

The first term on the right-hand side of (3.4) is bounded by the approximation error. Since $(\widehat{\Pi}^{(a/b)} - I)\widehat{p}^{(a/b)} = 0$, for all $\widehat{p}^{(a)} \in P_1$ and $\widehat{p}^{(b)} \in P_2$ respectively, the approximation error can be estimated by employing the Bramble-Hilbert Lemma [5] and the Deny-Lions Lemma [8].

Lemma 3.1. *Under the quasi-uniform assumption for $\mathcal{T}_h$, we have*

$$\inf_{v_h\in V_h} ||u-v_h||_h^{(a)} \le Ch|u|_{H^2(\Omega)}, \quad \inf_{v_h\in V_h} ||u-v_h||_h^{(b)} \le Ch^2|u|_{H^3(\Omega)}. \tag{3.5}$$

Proof. We take case (a) as example:

$$\begin{aligned}
\inf_{v_h\in V_h} ||u-v_h||_h &\le \sum_{K\in\mathcal{T}_h} |u-\Pi_K u|_{H^1(K)} \\
&\le C\sum_{K\in\mathcal{T}_h} ||B_K^{-1}|| \cdot |\det B_K|^{\frac{1}{2}} \cdot |\widehat{u} - \widehat{\Pi}_{\widehat{K}}\widehat{u}|_{H^1(\widehat{K})} \\
&\le C\sum_{K\in\mathcal{T}_h} ||B_K^{-1}|| \cdot |\det B_K|^{\frac{1}{2}} \cdot \inf_{\widehat{p}\in P_1(\widehat{K})} ||\widehat{u}+\widehat{p}||_{H^2(\widehat{K})} \\
&\le C\sum_{K\in\mathcal{T}_h} ||B_K^{-1}|| \cdot |\det B_K|^{\frac{1}{2}} \cdot |\widehat{u}|_{H^2(\widehat{K})} \\
&\le C\sum_{K\in\mathcal{T}_h} ||B_K^{-1}|| \cdot |\det B_K|^{\frac{1}{2}} \cdot ||B_K||^2 \cdot |\det B_K|^{-\frac{1}{2}} \cdot |u|_{H^2(K)} \\
&\le C\sum_{K\in\mathcal{T}_h} \rho_K^{-1} \cdot h_K^2 \cdot |u|_{H^2(K)} \le Ch|u|_{H^2(\Omega)},
\end{aligned}$$

where the third inequality follows by the Bramble-Hilbert Lemma and the fourth one by the Deny-Lions Lemma.

Now we are in a position to bound the second term on the right-hand side of (3.4), i.e., the consistency error. By Green's formula, we have

$$\begin{aligned}
a_h(u-u_h,w_h) &= \sum_{K\in\mathcal{T}_h} \int_K \nabla u\cdot\nabla w_h d\sigma - \int_\Omega f w_h d\sigma \\
&= \sum_{K\in\mathcal{T}_h} \{\int_{\partial K} \frac{\partial u}{\partial \nu} w_h ds - \int_K (\Delta u) w_h d\sigma\} - \int_K f w_h d\sigma \\
&= \sum_{K\in\mathcal{T}_h} \int_{\partial K} \frac{\partial u}{\partial \nu} w_h ds \\
&= \sum_{\substack{F\,\in\,\partial\mathcal{T}_h \\ F\,\not\subset\,\partial\Omega}} \int_F \frac{\partial u}{\partial \nu}[w_h]_F ds + \sum_{F\subset\partial\Omega} \int_F \frac{\partial u}{\partial \nu} w_h ds,
\end{aligned} \tag{3.6}$$

where $[\,\cdot\,]_F$ denote the jump over element side F. Since for any $w_h \in V_h$,

$$P_0^F([w_h]_F) = 0, \quad \text{if } F \not\subset \partial\Omega, \quad \text{and} \quad P_0^F(w_h) = 0, \quad \text{if } F \subset \partial\Omega,$$

we have for $F \in \partial\mathcal{T}_h, F \not\subset \partial\Omega$, the following equality holds

$$\int_F \frac{\partial u}{\partial \nu}[w_h]_F ds = \int_F \frac{\partial u}{\partial \nu} R_0^F([w_h]_F) ds = \int_F R_0^K(\frac{\partial u}{\partial \nu}) R_0^F([w_h]_F) ds.$$

Thus by Schwarz's inequality,

$$\begin{aligned} |\int_F \frac{\partial u}{\partial \nu}[w_h]_F ds| &\leq \int_F |R_0^K(\frac{\partial u}{\partial \nu}) R_0^F([w_h]_F)| ds \\ &\leq ||R_0^K(\frac{\partial u}{\partial \nu})||_{L^2(F)} \cdot ||R_0^F([w_h]_F)||_{L^2(F)}. \end{aligned} \tag{3.7}$$

Lemma 3.2.

$$||R_0^K(v)||_{L^2(\partial K)} \leq Ch^{1/2}|v|_{H^1(K)}, \quad \forall v \in H^1(K).$$

Proof. Employing the Trace Theorem on the reference element $\widehat{K}$, we have

$$\begin{aligned} ||R_0^K(v)||^2_{L^2(\partial K)} &\leq Ch||\widehat{R_0^K(v)}||^2_{L^2(\partial\widehat{K})} \leq Ch||\widehat{R_0^K(v)}||^2_{H^1(\widehat{K})} \\ &= Ch\{||\widehat{R_0^K(v)}||^2_{L^2(\widehat{K})} + |\widehat{R_0^K(v)}|^2_{H^1(\widehat{K})}\} \\ &\leq C\{h^{-1}||R_0^K(v)||^2_{L^2(K)} + h|R_0^K(v)|^2_{H^1(K)}\} \\ &\leq Ch|v|^2_{H^1(K)}, \end{aligned}$$

which completes the proof.

Use the above lemma, we have

$$||R_0^K(\frac{\partial u}{\partial \nu})||_{L^2(F)} \leq Ch^{1/2}|\frac{\partial u}{\partial \nu}|_{H^1(K)} \leq Ch^{1/2}|u|_{H^2(K)}, \tag{3.8}$$

$$\begin{aligned} ||R_0^F([w_h]_F)||_{L^2(F)} &= ||R_0^F(w_h|_{K_+} - w_h|_{K_-})||_{L^2(F)} \\ &\leq \{||R_0^F(w_h|_{K_+})||_{L^2(F)} + ||R_0^F(w_h|_{K_-})||_{L^2(F)}\} \\ &\leq C\{||R_0^{K_+}(w_h)||_{L^2(F)} + ||R_0^{K_-}(w_h)||_{L^2(F)}\} \\ &\leq Ch^{1/2}\{|w_h|_{H^1(K_+)} + |w_h|_{H^1(K_-)}\}, \end{aligned} \tag{3.9}$$

where F is the common edge of the elements K_+ and K_-.

Substituting (3.8)-(3.9) into (3.7) (summation over $F \not\subset \partial\Omega$), we get

$$\sum_{\substack{F \in \partial\mathcal{T}_h \\ F \not\subset \partial\Omega}} |\int_F \frac{\partial u}{\partial \nu}[w_h]_F ds| \leq \sum_{K \in \mathcal{T}_h} Ch|u|_{H^2(K)}|w_h|_{H^1(K)} \leq Ch|u|_{H^2(\Omega)}||w_h||_h. \tag{3.10}$$

Analogously, for $F \subset \partial\Omega$, we have

$$\sum_{F \subset \partial\Omega} |\int_F \frac{\partial u}{\partial \nu} w_h ds| \leq Ch|u|_{H^2(\Omega)}||w_h||_h. \tag{3.11}$$

By (3.10)-(3.11) and (3.6), we can get

$$|a_h(u - u_h, w_h)| \leq Ch|u|_{H^2(\Omega)}||w_h||_h. \tag{3.12}$$

Theorem 3.1. *Suppose $u \in H^2(\Omega)$, under the quasi-uniform partition $\mathcal{T}_h$ mentioned above, we have the following error estimates:*

$$h||u - u_h||_h + ||u - u_h||_{L^2(\Omega)} \leq Ch^2|u|_{H^2(\Omega)}. \tag{3.13}$$

Proof. Employing Lemma 3.1 and substituting (3.12) into (3.4), we obtain

$$||u - u_h||_h^{(a/b)} \leq Ch|u|_{H^2(\Omega)}.$$

By the Aubin-Nitsche duality argument in standard finite element theory [1], we can get

$$||u - u_h||_{L^2(\Omega)}^{(a/b)} \leq Ch^2|u|_{H^2(\Omega)}.$$

Then the proof is complete.

4. Numerical Experiment

In order to investigate the numerical behavior of the two hexagonal elements, we consider the second order problem (3.1) with

$$f(x, y) = -2(y + x\cot\theta_3) + 2\cot\theta_2(x + 3y\cot\theta_3 - \sin\theta_1).$$

And Ω is a triangular domain consisted by $l_1 : y = 0$, $l_2 : y = (\sin\theta_1 - x)\tan\theta_3$, and $l_3 : y = x\tan\theta_2$, where $\theta_1, \theta_2, \theta_3$ are the three inner angles of Ω. It can be verified that the exact solution of problem (3.1) is

$$u(x, y) = y(x - y\cot\theta_2)(x + y\cot\theta_3 - \sin\theta_1).$$

We equally divide the three edges of Ω into N segments and partition Ω with small hexagons and a few triangles near the boundary. The meshes obtained in this way for $N = 9$ and $N = 18$ are illustrated in Fig. 4.1.

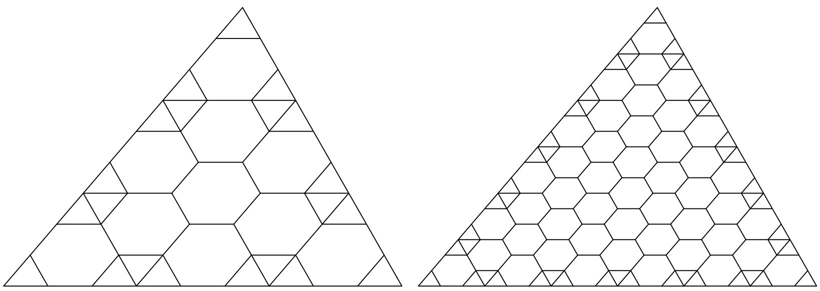

Fig. 4.1. The hexagonal meshes for the triangular domain Ω (left: $N = 9$, right: $N = 18$).

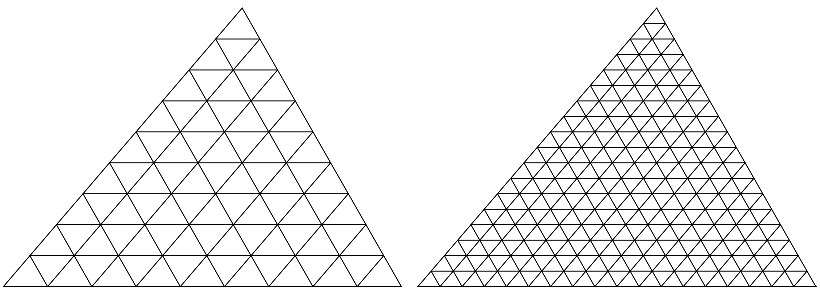

Fig. 4.2. The triangular meshes for the triangular domain Ω (left: $N = 9$, right: $N = 18$).

Table 4.1: Errors in energy norm using element-(a): $||u - u_h||_h$.

N	DOF	$(60°, 60°, 60°)$		$(45°, 60°, 75°)$		$(20°, 50°, 110°)$	
18	183	$8.758 * 10^{-3}$	–	$6.441 * 10^{-3}$	–	$1.349 * 10^{-3}$	–
36	696	$4.450 * 10^{-3}$	1.97	$3.249 * 10^{-3}$	1.98	$6.207 * 10^{-4}$	2.17
72	2694	$2.241 * 10^{-3}$	1.99	$1.630 * 10^{-3}$	1.99	$2.922 * 10^{-4}$	2.12
144	10578	$1.124 * 10^{-3}$	1.99	$8.160 * 10^{-4}$	2.00	$1.409 * 10^{-4}$	2.07

Table 4.2: Errors in energy norm using element-(b): $||u - u_h||_h$.

N	DOF	$(60°, 60°, 60°)$		$(45°, 60°, 75°)$		$(20°, 50°, 110°)$	
18	229	$3.161 * 10^{-3}$	–	$2.540 * 10^{-3}$	–	$1.064 * 10^{-3}$	–
36	895	$1.329 * 10^{-3}$	2.37	$1.078 * 10^{-3}$	2.36	$4.765 * 10^{-4}$	2.23
72	3523	$5.721 * 10^{-4}$	2.32	$4.689 * 10^{-3}$	2.30	$2.194 * 10^{-4}$	2.17
144	13963	$2.568 * 10^{-4}$	2.29	$2.125 * 10^{-4}$	2.21	$1.042 * 10^{-4}$	2.11

Table 4.3: Errors in energy norm using C-R element: $||u - u_h||_h$.

N	DOF	$(60°, 60°, 60°)$		$(45°, 60°, 75°)$		$(20°, 50°, 110°)$	
18	459	$6.846 * 10^{-3}$	–	$5.496 * 10^{-3}$	–	$2.373 * 10^{-3}$	–
36	1890	$3.426 * 10^{-3}$	2.00	$2.750 * 10^{-3}$	2.00	$1.190 * 10^{-3}$	1.99
72	7668	$1.713 * 10^{-3}$	2.00	$1.376 * 10^{-3}$	2.00	$5.960 * 10^{-4}$	2.00
144	30888	$8.566 * 10^{-3}$	2.00	$6.880 * 10^{-4}$	2.00	$2.982 * 10^{-4}$	2.00

Table 4.4: Errors in L^2 norm using element-(a): $||u - u_h||_{L^2(\Omega)}$.

N	DOF	$(60°, 60°, 60°)$		$(45°, 60°, 75°)$		$(20°, 50°, 110°)$	
18	183	$1.441 * 10^{-4}$	–	$1.017 * 10^{-4}$	–	$1.581 * 10^{-5}$	–
36	696	$3.740 * 10^{-5}$	3.85	$2.621 * 10^{-5}$	3.88	$3.650 * 10^{-6}$	4.33
72	2694	$9.551 * 10^{-6}$	3.92	$6.663 * 10^{-6}$	3.93	$8.589 * 10^{-7}$	4.25
144	10578	$2.414 * 10^{-6}$	3.96	$1.680 * 10^{-6}$	3.97	$2.068 * 10^{-7}$	4.15

Table 4.5: Errors in L^2 norm using element-(b): $||u - u_h||_{L^2(\Omega)}$.

N	DOF	$(60°, 60°, 60°)$		$(45°, 60°, 75°)$		$(20°, 50°, 110°)$	
18	229	$3.821 * 10^{-5}$	–	$3.016 * 10^{-5}$	–	$1.241 * 10^{-5}$	–
36	895	$8.184 * 10^{-6}$	4.67	$6.521 * 10^{-6}$	4.63	$2.824 * 10^{-6}$	4.40
72	3523	$1.793 * 10^{-6}$	4.56	$1.443 * 10^{-6}$	4.52	$6.580 * 10^{-7}$	4.30
144	13963	$4.089 * 10^{-7}$	4.38	$3.321 * 10^{-7}$	4.35	$1.575 * 10^{-7}$	4.18

Table 4.6: Errors in L^2 norm using C-R element: $||u - u_h||_{L^2(\Omega)}$.

N	DOF	$(60°, 60°, 60°)$		$(45°, 60°, 75°)$		$(20°, 50°, 110°)$	
18	459	$7.667 * 10^{-5}$	–	$6.118 * 10^{-5}$	–	$2.839 * 10^{-5}$	–
36	1890	$1.918 * 10^{-5}$	4.00	$1.533 * 10^{-5}$	4.00	$7.162 * 10^{-6}$	3.96
72	7668	$4.797 * 10^{-6}$	4.00	$3.834 * 10^{-6}$	4.00	$1.795 * 10^{-6}$	3.99
144	30888	$1.199 * 10^{-6}$	4.00	$9.582 * 10^{-7}$	4.00	$4.492 * 10^{-7}$	4.00

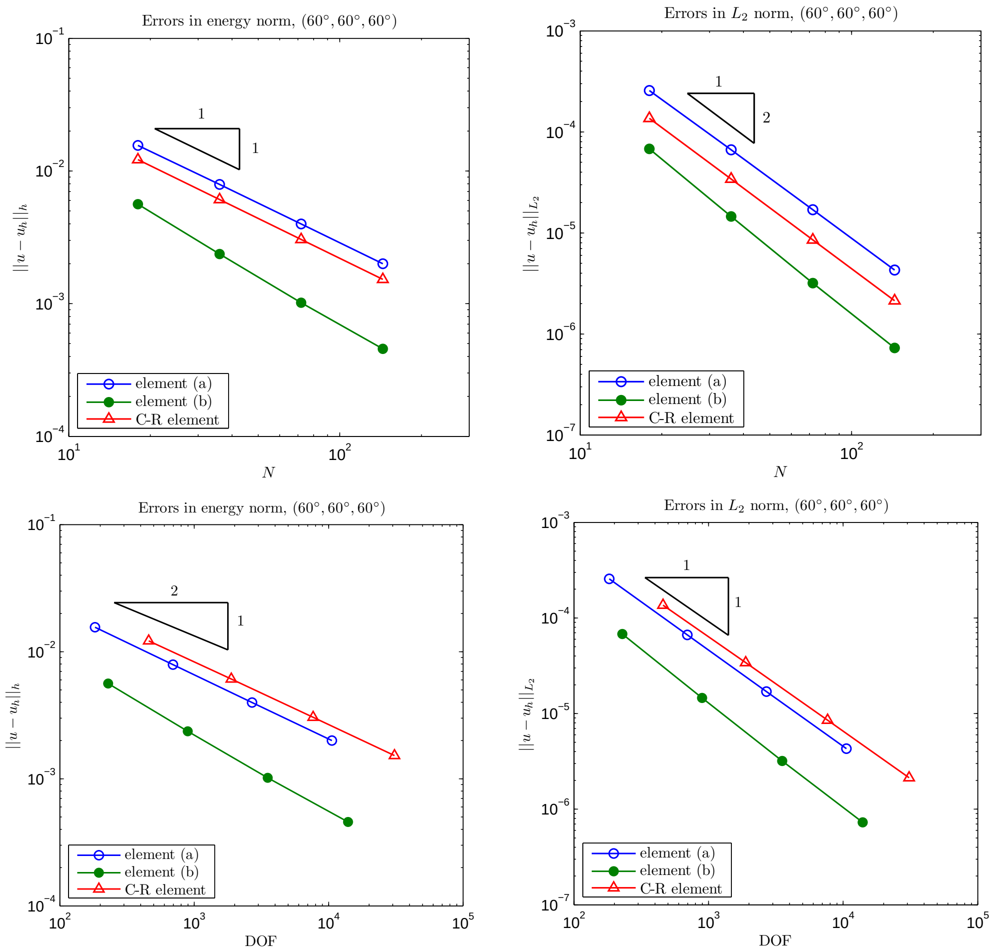

Fig. 4.3. Comparisons among the Q_1 hexagonal element (element (a)), the modified Q_1 hexagonal element (element (b)), and the Crouzeix-Raviart triangular element (C-R element).

We give the numerical results of the above problem using our nonconforming hexagonal elements. And we also use the famous Crouzeix-Raviart element (see [7]) for the sake of comparison upon the triangular mesh illustrated in Fig. 4.2. A variety of different inner angles $(\theta_1, \theta_2, \theta_3)$ of Ω are considered. In Tables 4.1-4.3, we list the results in the energy norm for the Q_1 hexagonal element, the modified Q_1 hexagonal element and the Crouzeix-Raviart element respectively. And in Tables 4.4-4.6, the corresponding results in the L_2 norm are given.

The results show that both of the new hexagonal elements are convergent with first order in energy norm and second order in L_2 norm, comparable with the Crouzeix-Raviart element. Although the Q_1 hexagonal element is slightly inaccurate, nearly 2/3 of the degree of freedoms are saved. And the modified hexagonal element is more accurate than the Crouzeix-Raviart element with more than 1/2 degree of freedoms saved. Fig. 4.3 gives a more clear illustration for the case of $(\theta_1, \theta_2, \theta_3) = (60°, 60°, 60°)$. One may be concerned about which is the most accurate among the three elements with a given number of degrees of freedom. From the two log-log plots on the bottom of Fig. 4.3, we can see that both hexagonal elements achieve better accuracy than the Crouzeix-Raviart element.

Acknowledgments. The authors would like to thank Prof. Jinchao Xu and Prof. Xuejun Xu for fruitful discussions. Thanks are also given to the anonymous referees for helpful suggestions and the editors for improvement of the English in the manuscript.

References

[1] S.C. Brenner, L.R. Scott, The Mathematical Theory of Finite Element Methods, Springer-Verlag, New York, 1994.

[2] P.G. Ciarlet, The Finite Element Method for Elliptic Problems, North-Holland Publishing Company, Amsterdam, New York, Oxford, 1976.

[3] G.C. Sih, V.P. Tamuzh (eds.), Fracture of Composite Materials, Proc. II Soviet-American Symp., Martinus Nijhoff Publ., The Hague-Boston-London, 1982.

[4] R. Williams, The Geometrical Foundation of Natural Structure: A Source Book of Design, Dover, New York, 1979, 35-43.

[5] J.H. Bramble, S.R. Hilbert, Estimation of linear functionals on Sobolev spaces with application to fourier transforms and spline interpolation, *SIAM J. Numer. Anal.*, **7**:1 (1970), 112-124.

[6] Z.Q. Cai, J. Douglas Jr., X. Ye, A stable nonconforming quadrilateral finite element method for the stationary Stokes and Navier-Stokes equations, *Calcolo*, **36** (1999), 215-232.

[7] M. Crouzeix, P.A. Raviart, Conforming and non-conforming finite elements for solving the stationary Stokes equations, *R.A.I.R.O. Anal. Numér.*, **7** (1973), 33-76.

[8] J. Deny, J.L. Lions, Les espaces du type Beppo-Levi, *Annales de l'Institut Fourier (Grenoble)*, **5** (1955), 305-370.

[9] J. Douglas Jr., J.E. Santos, D. Sheen, X. Ye, Nonconforming Galerkin methods based on quadrilateral elements for second order elliptic problems, *R.A.I.R.O. Modél. Math. Anal. Numér.,* **33** (1999), 747-770.

[10] J.L. Gout, Rational Wachspress-type finite elements on regular hexagons, *IMA J. Numer. Anal.*, **5** (1985), 59-77.

[11] H.D. Han, Nonconforming elements in the mixed finite element method, *J. Comput. Math.*, **2** (1984), 223-233.

[12] M. Ishiguro, Construction of hexagonal basis functions applied in the Galerkin-type finite element method, *J. Inf. Proc.*, **7**:2 (1984), 89-95.

[13] M. Ishiguro, K. Higuchi, Application of hexagonal finite element nethod to three-dimensitional diffusion problem of fast reactors, *J. Nuc. Sci. Tech.*, **20**:11 (1983), 951-960.

[14] R. Rannacher, S. Turek, Simple nonconforming quadrilateral Stokes element, *Numer. Meth. PDEs.*, **8** (1992), 97-111.

[15] Z.C. Shi, The generalized patch test for Zienkiewicz's triangles, *J. Comput. Math.*, **2** (1984), 279-286.

[16] Z.C. Shi, Convergence properties of two nonconforming finite elements, *Comput. Methods Appl. Mech. Engrg.*, **48** (1985), 123-139.

[17] N. Sukumar, A. Tabarraei, Conforming polygonal finite elements, *Int. J. Numer. Meth. Engng.*, **61** (2004), 2045-2066.

[18] J.C. Sun, Multivariate Fourier series over a class of non tensor-product partition domains, *J. Comput. Math.*, **12**:1 (2003), 53-62.

[19] J.C. Sun, C. Yang, On construction of difference schemes and finite elements over hexagon partitions, Current Trends in High Performance Computing and its Applications, Edited by W. Zhang, et al., Springer-Verlag, 123-135, 2005.